Mon. Not. R. Astron. Soc. **306,** 473–478 (1999)

Electron-impact rotational excitation of CH^+

Andrew J. Lim, Ismanuel Rabadán and Jonathan Tennyson★
Department of Physics and Astronomy, University College London, Gower Street, London WC1E 6BT

Accepted 1999 February 4. Received 1999 January 22; in original form 1998 October 7

ABSTRACT

New coupled-state **R**-matrix calculations are performed at energies up to 1 eV to give rotational excitation and de-excitation cross-sections for electron collisions with CH^+. Rotational excitations with Δj up to 7 are considered. Transitions with Δj up to 6 are found to have appreciable cross-sections, those with $\Delta j = 2$ being comparable to (indeed slightly larger than) those with $\Delta j = 1$, the only ones considered previously. Rates for electron temperatures up to 15 000 K and critical electron densities are given. A model of CH^+ rotational populations shows them to be relatively insensitive to electron temperatures in the range 800–2000 K, but to depend strongly upon electron density. The models predict a significant population in rotational states with $j > 1$ even at low electron densities; at higher densities the possibility exists that electron collisions alone might explain the recently observed populations in the planetary nebula NGC 7027.

Key words: molecular data – molecular processes – planetary nebulae: individual: NGC 7027.

1 INTRODUCTION

CH^+ was the first ever molecular ion to be observed in the interstellar medium, via its optical spectrum. Observations of CH^+ have persistently given abundances greater, by as much as two orders of magnitude, than corresponding theoretical models. Attempts to resolve this discrepancy continue (Federman et al. 1996; Chieze, Pineaux des Forêts & Flower 1998).

Recent observations of the planetary nebula NGC 7027 using *ISO* have, for the first time, recorded pure rotational spectra of CH^+ (Cernicharo et al. 1997). Transitions were observed for $j' - j$ equal to 2–1, 3–2, 4–3, 5–4 and 6–5. Conventional wisdom (Neufeld & Dalgarno 1989) is that excitation of molecular ions at low densities is dominated by collisions with electrons. This is because the cross-sections for electron-impact excitation of molecular ions are several orders of magnitude larger than the corresponding ones for excitation by atomic or molecular collision partners such as H or H_2.

There are essentially no experimental determinations of electron-impact excitation rates for molecular ions, so astronomical models have relied exclusively on theoretical estimates for these parameters. There have been a number of theoretical determinations of electron-impact excitation rates for CH^+ (Chu & Dalgarno 1974; Dickinson & Muñoz 1977; Flower 1979; Dickinson & Flower 1981; Neufeld & Dalgarno 1989). These studies have all been highly approximate. The most commonly used method for obtaining rotational excitation rates has been the Coulomb–Born approximation (Boĭkova & Ob''edkov 1968; Chu & Dalgarno 1974; Flower 1979; Neufeld & Dalgarno 1989), which assumes that all collisional excitation is due entirely to long-range effects. For CH^+ it has always been assumed that only dipolar interactions need to be considered. Within this model, and indeed the other cited above, only single jumps in vibrational or rotational quanta are possible.

Recent **R**-matrix studies on HeH^+ and NO^+ (Rabadán, Sarpal & Tennyson 1998a,b) have suggested that the (dipole) Coulomb–Born approximation is not a reliable method for computing electron-impact rotational excitation rates. In particular, a more complete treatment can lead to significant population of higher rotational states, particularly $j = 2$. In this work we present rotational electron-impact excitation rates for CH^+ that should be significantly more reliable than those given previously. We use these to model CH^+ rotational emission spectra using conditions similar to those thought to prevail in NGC 7027.

2 CALCULATIONS

2.1 R-matrix calculations

One of us (Tennyson 1988) has previously performed an **R**-matrix-based study of electron – CH^+ collisions. However, this study used a crude, self-consistent field (SCF), representation of both the target and low-lying electronically excited states of the system, and was not considered to be sufficiently accurate for the present work.

New calculations were therefore performed using the UK molecular **R**-matrix package (Gillan, Tennyson & Burke 1995; Morgan, Tennyson & Gillan 1998). Calculations were performed at the single, fixed equilibrium CH^+ bondlength of 2.137 a_0 using an **R**-matrix radius of 10 a_0. A fixed bondlength is appropriate, as previous studies on HeH^+ and NO^+ have shown that electron-impact rotational excitation cross-sections are rather insensitive to vibrational motion effects (Rabadán et al. 1998a).

★Author to whom correspondence should be addressed; e-mail: j.tennyson@ucl.ac.uk

We represent the CH^+ molecular ion with a basis consisting of 28 Slater-type orbitals (STOs) distributed in the following symmetries: 16σ, 8π, 3δ, 1ϕ, taken from Cade & Huo (1973). Six CH^+ target states, the lowest states of symmetry $^1\Sigma^+$, $^3\Pi$, $^1\Pi$, $^3\Sigma^-$, $^1\Delta$ and $^3\Sigma^+$, were included in the close-coupling expansion. These were generated using a complete active space configuration interaction (CASCI) procedure (Tennyson 1996) in which the six electrons of the CH^+ ion are distributed according to the prescription, $1\sigma^2\{2\sigma 3\sigma 4\sigma 2\pi\}^4$. All six target states were considered in both the inner and outer region of the calculation.

This model gives a ground-state dipole moment for CH^+ of 1.543 D at 2.173 a_0. This should be compared the best available (theoretical) value of 1.655 D (Ornellas & Machado 1986) for the CH^+ vibrational ground state.

We represent the continuum with 203 numerically calculated basis orbitals with $l \leq 8$, $m \leq 3$ and energy less than 9 Ryd. These were Lagrange- and then Schmidt-orthogonalized to the CH^+ target orbitals (Tennyson, Burke & Berrington 1987). This calculation was performed for the total symmetries $^2\Sigma$, $^2\Pi$, $^2\Delta$ and $^2\Phi$. At each energy, the four resulting fixed nuclei **T**-matrices are used to calculate the pure rotational cross-sections, following the recommended procedure of Rabadán et al. (1998a), as implemented in program ROTIONS (Rabadán & Tennyson 1998). In this procedure, higher partial wave contributions to the $\Delta j = 1$ transitions are computed using the Coulomb–Born approximation, whereas transitions with $\Delta j > 1$ are obtained using the four fixed nuclei **T**-matrices. Particularly at low energies, the effect of energy changes at threshold can become important. These can only be included rigorously in a full rotational close-coupling calculation, which is not practical at the collision energies studied here because of the large number of channels that would be involved. Instead, the computed cross-sections were threshold-corrected using kinematic ratios (Chandra & Temkin 1976).

Scattering calculations were performed up to a collision energy of 1 eV. Above this value, the contribution to the rates was estimated using the same high-energy tail procedure as Rabadán et al. (1998b). The relatively low energy cut-off for our full calculations was caused by the need to avoid threshold of the first electronically excited state of CH^+, a $^3\Pi$, at 1.2 eV. This state also introduces a series of Rydberg resonances into our computed cross-sections. Unlike the narrow, nuclear-excited Feshbach resonances which are introduced with vibrational motion and whose influence has been found to be small (Rabadán et al. 1998a), some of these Feshbach resonances are relatively broad. Cross-sections were therefore computed on a fine energy grid, so that the effect of these resonances could be included in the calculations.

3 RESULTS AND DISCUSSION

Pure rotational cross-sections are found for all transitions $j \rightarrow j'$, for $j = 0, 1, 2, 3, 4, 5$ and 6 and $j' = 1, 2, 3, 4, 5, 6$ and 7. Shown in Fig. 1 are cross-sections for excitation from the rotational ground state. A notable feature of Fig. 1 is the presence of many narrow resonances which converge on the electronically excited states of CH^+. A full study of these resonances, including their behaviour as a function of internuclear separation, is presently in progress.

Rates of rotational excitation were obtained assuming a Maxwellian velocity distribution for the electrons. Results for excitations starting from the rotational ground state are given in Fig. 2 which shows that electron-impact excitation rates for $j = 0 \rightarrow 2$ actually exceed those for $j = 0 \rightarrow 1$ at all temperatures considered. This is contrary to all previous assumptions about this process. Significant rates are found for processes up to $j = 0 \rightarrow 6$; however, the $j = 0 \rightarrow 7$ rates are too small to include on the figure.

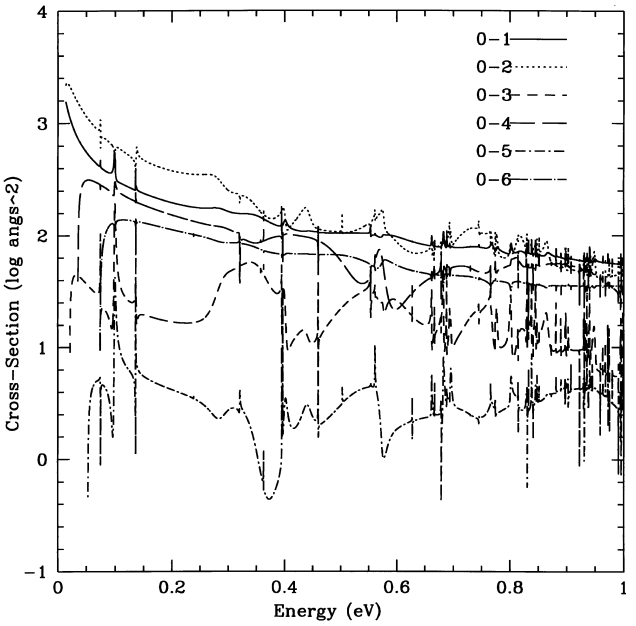

Figure 1. Cross-sections for rotational excitation of CH^+ from the ground state to the lowest six excited states.

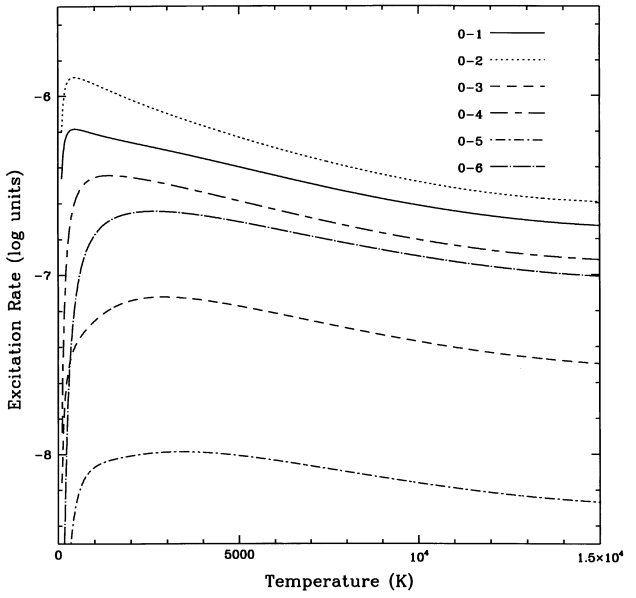

Figure 2. Rotational excitation rates (in $cm^3\ s^{-1}$) for CH^+ corresponding to the cross-sections shown in Fig. 1.

For ease of use in modelling, the temperature dependence of the rates, q, for the important transitions have been fitted using the form

$$q_{j \rightarrow j'}(T) = a(T)^{b + c \ln(T)}, \quad (1)$$

where T is in Kelvin and q is in $cm^3\ s^{-1}$. This form is different from the one used in our previous studies (Sarpal & Tennyson 1993; Rabadán et al. 1998b), as the resonances discussed above alter the temperature dependence of the rate coefficients. The fitted parameters for these processes are given in Table 1. All fits reproduce our data to within 4 per cent. Rates for the de-excitation process can

Table 1. Fitted parameters to the rate coefficients. Rates were fitted to equation (1).

Transition	a	b	c
j = 0-1	2.48522(−9)	1.71024	−0.131293
j = 0-2	3.12982(−9)	1.90998	−0.152223
j = 0-3	4.30991(−15)	4.267	−0.273132
j = 0-4	1.09957(−12)	3.45176	−0.234753
j = 0-5	2.13364(−15)	3.88253	−0.244649
j = 0-6	4.90262(−16)	5.05041	−0.319809
j = 0-7	3.04347(−20)	6.24875	−0.382721
j = 1-0	8.50751(−10)	1.70465	−0.130989
j = 1-2	9.51699(−10)	1.8132	−0.136176
j = 1-3	2.86131(−10)	2.38589	−0.178111
j = 1-4	4.22873(−16)	4.68508	−0.296508
j = 1-5	4.96852(−14)	4.10057	−0.269496
j = 1-6	2.52460(−17)	4.81587	−0.297974
j = 1-7	1.76759(−17)	5.61254	−0.34773
j = 2-0	6.68550(−10)	1.89658	−0.151517
j = 2-1	6.03522(−10)	1.80132	−0.135524
j = 2-3	4.85726(−10)	1.91768	−0.14216
j = 2-4	3.00331(−11)	2.86783	−0.204729
j = 2-5	2.45679(−17)	5.2895	−0.331041
j = 2-6	2.55269(−15)	4.6635	−0.29929
j = 2-7	1.04596(−18)	5.43036	−0.330723
j = 3-0	5.91067(−16)	4.27997	−0.274047
j = 3-1	1.25315(−10)	2.38546	−0.1783
j = 3-2	3.75743(−10)	1.90056	−0.141219
j = 3-4	1.82091(−10)	2.15951	−0.156141
j = 3-5	3.01053(−13)	3.86219	−0.260495
j = 3-6	2.66224(−18)	5.75837	−0.357393
j = 3-7	2.17031(−16)	5.15401	−0.325884
j = 4-0	1.33266(−13)	3.43549	−0.233964
j = 4-1	1.62940(−16)	4.65336	−0.294739
j = 4-2	1.68640(−11)	2.87071	−0.205139
j = 4-3	1.55094(−10)	2.14016	−0.155086
j = 4-5	4.71653(−11)	2.45704	−0.173493
j = 4-6	6.60275(−13)	3.66061	−0.248929
j = 4-7	4.46313(−19)	6.13641	−0.378499
j = 5-0	1.92809(−16)	3.89007	−0.245342
j = 5-1	1.50216(−14)	4.0812	−0.268535
j = 5-2	1.27822(−17)	5.26089	−0.329475
j = 5-3	1.73460(−13)	3.89185	−0.262519
j = 5-4	4.24313(−11)	2.43712	−0.17242
j = 5-6	1.39307(−11)	2.72452	−0.188936
j = 5-7	1.15303(−13)	4.0528	−0.272255
j = 6-0	4.21847(−17)	5.02923	−0.318755
j = 6-1	6.41741(−18)	4.79872	−0.297185
j = 6-2	7.66908(−16)	4.73656	−0.304364
j = 6-3	1.66155(−18)	5.72728	−0.35569
j = 6-4	4.28344(−13)	3.68325	−0.250583
j = 6-5	1.22598(−11)	2.71877	−0.188765
j = 6-7	5.32507(−13)	3.6913	−0.262788
j = 7-0	3.75257(−21)	6.10703	−0.374468
j = 7-1	8.44757(−19)	5.9645	−0.369043
j = 7-2	4.00679(−19)	5.40386	−0.329398
j = 7-3	1.12253(−16)	5.13561	−0.325004
j = 7-4	3.08272(−19)	6.10705	−0.376908
j = 7-5	8.01487(−14)	4.07279	−0.273746
j = 7-6	5.43213(−13)	3.65313	−0.260487

be computed using the principle of detailed balance (see e.g., Dickinson & Muñoz 1977 and Dickinson & Flower 1981). We note that the kinematic scaling used to get the correct threshold behaviour makes it difficult to obtain simple relationships between excitation and de-excitation rates for the same process.

Table 2 shows the critical electron densities calculated using

$$n_{\rm cr}(j';T) = \frac{A_{j'\rightarrow j'-1}}{q_{j'\rightarrow j}(T)} \ . \qquad (2)$$

The Einstein coefficients for spontaneous emission, $A(j' \rightarrow j)$, were calculated from the dipole moment using the method of Neufeld & Dalgarno (1989). In determining $n_{\rm cr}(j';T)$ we consider only the transitions $q_{0\rightarrow j'}(T)$. This is correct for $j' = 1$, but for states with $j' > 1$ this value is an upper limit on the critical density due to the existence of alternative excitation paths whose importance depends on the electron density, $n_{\rm e}$.

4 THE NUMERICAL MODEL OF NGC 7027

We have constructed a simple numerical model of the excitation of pure rotational levels of CH^+ molecular ions in an astrophysical situation, such as that found in a planetary nebula. The pure rotational spectrum of CH^+ has been identified in the far-infrared emission of NGC 7027 by Cernicharo et al. (1997), and so we have used typical inferred physical conditions for this nebula in the model (Liu et al. 1996; Liu 1997). This implies a number density of hydrogen nuclei of order 10^5, an $n_{\rm e}/n_{\rm H}$ value of order 3×10^{-4}, and an electron temperature in the region of 1000 K.

Using the rotational excitation rates and Einstein A coefficients calculated above, the steady-state populations of the rotational levels can be found by integrating the equation

$$\frac{{\rm d}n_k}{{\rm d}t} = \sum_{i\neq k} n_{\rm e} q_{i\rightarrow k}(T) n_i - A_{k\rightarrow k-1} n_k - \sum_{i\neq k} n_{\rm e} q_{k\rightarrow i}(T) n_k . \qquad (3)$$

In this equation, n_k is the population of the rotational level with quantum number k, and $n_{\rm e}$ is the local electron density. The first term in this equation describes transitions to the state k from all other states i, the second term describes spontaneous decay, and the third term describes depopulation due to transitions from the state k to all other states i. This equation gives the rate of change of occupancy for a single j-level; in our models we consider values of j between 0 and 7.

In order to obtain the steady-state level populations, a series of computational bins are constructed to represent rotational levels $j = 0 - 7$, and the conditions at time $t = 0$ are imposed as follows: $n_0 = 1.0$ and $n_{j>0} = 0.0$. Equation (3) can then be applied to find ${\rm d}n_j/{\rm d}t$ for all values of j, and the system is marched forward in time (ensuring the time-step was small enough for numerical stability) until a steady state is reached.

The final steady configuration is found to be independent of the initial conditions, as can be seen by considering equation (3) with the left-hand side set to zero. This independence of the initial state of the ion is consistent within our model, but exposes one of its important limitations. We are considering a static population of CH^+, whereas in a real situation there will be a 'turn-over' as the chemistry of, say, a diffuse cloud proceeds. It is likely that CH^+ is formed in higher rotational levels and cross-sections for its destruction, especially by electron impact via dissociative recombination, must also depend on the state of the target.

Whether these effects have a strong influence on the rotational emission spectrum will depend on the mean lifetime of a CH^+ ion; neither, however, are currently included in our simple model.

Initially, three models were constructed: model A includes only transitions with $\Delta j = 1$, model B considers only excitations from the $j = 0$ level to the $j = 1 - 7$ levels, and model C considers all excitations between the $j = 0$ and $j = 7$ levels.

Table 2. Critical electron density, n_{cr} in cm^{-3}, as a function of temperature, for rotational levels. Powers of 10 are given in parentheses.

T(K)	$j = 1$	$j = 2$	$j = 3$	$j = 4$	$j = 5$	$j = 6$
100	1.90(4)	9.91(4)	3.26(7)	4.21(7)	3.00(10)	1.98(10)
200	1.15(4)	5.73(4)	1.06(7)	5.96(6)	1.35(9)	2.88(8)
300	1.03(4)	5.08(4)	7.33(6)	3.22(6)	4.65(8)	7.20(7)
400	1.00(4)	4.93(4)	6.10(6)	2.41(6)	2.78(8)	3.65(7)
500	1.00(4)	4.93(4)	5.46(6)	2.05(6)	2.08(8)	2.45(7)
1000	1.06(4)	5.37(4)	4.08(6)	1.60(6)	1.31(8)	1.17(7)
2000	1.19(4)	6.59(4)	3.16(6)	1.59(6)	1.14(8)	8.85(6)
3000	1.32(4)	7.89(4)	3.02(6)	1.74(6)	1.09(8)	8.70(6)
4000	1.47(4)	9.26(4)	3.15(6)	1.94(6)	1.09(8)	9.18(6)
5000	1.64(4)	1.07(5)	3.40(6)	2.17(6)	1.14(8)	9.95(6)
6000	1.83(4)	1.23(5)	3.73(6)	2.42(6)	1.21(8)	1.09(7)
7000	2.04(4)	1.40(5)	4.10(6)	2.70(6)	1.30(8)	1.20(7)
8000	2.25(4)	1.57(5)	4.50(6)	2.99(6)	1.40(8)	1.31(7)
9000	2.47(4)	1.74(5)	4.92(6)	3.28(6)	1.50(8)	1.43(7)
10000	2.69(4)	1.91(5)	5.35(6)	3.58(6)	1.61(8)	1.55(7)
15000	3.49(4)	2.46(5)	7.09(6)	4.62(6)	2.06(8)	2.00(7)
20000	3.52(4)	2.37(5)	7.44(6)	4.59(6)	2.15(8)	2.02(7)

Steady-state rotational populations were calculated with models A, B and C using the typical densities for NGC 7027 quoted above, and a range of electron temperatures between 800 and 2000 K in steps of 100 K. In these models we set the number density of CH^+ to unity; the populations we obtain are therefore those per particle. The emission rates are trivially calculated as the product of the level populations with the relevant Einstein A coefficients, and the results of these simulations are shown in Fig. 3 as plots of number rate of emissions against electron temperature. It can be seen from this figure that, within the range considered, the temperature dependence of the level populations is very weak; this is a result of the fact that the peak-decay structure of the rate curves occurs over a scale of the order of 10 000 K; see Fig. 2. A range of size 1000 K therefore displays little structure.

The primary excitation paths within the system are also apparent from Fig. 3. The results of models B and C are almost identical, demonstrating that, at this electron density, most of the excitations take place through transitions from the $j = 0$ level. This is a direct result of the low level of excitation in the models, with approximately 99 per cent of the ions being in the ground rotational state. In this situation, excitation from the $j = 0$ level is the dominant pathway to the higher levels, simply due to the large number of ions in the ground state.

Model A is based on the standard assumption of $\Delta j = 1$ excitations only. Our results show that this approach, as expected, makes a negligible contribution to populating the higher levels.

Tables 3 and 4 show the fluxes of CH^+ pure-rotational emission which has recently been detected from NGC 7027 by Cernicharo et al. (1997). These are calculated as the number of emissions relative to the $j = 2 - 1$ transition by a simple manipulation of the energy fluxes given in the cited paper. Shown in Table 3 is the corresponding steady-state emission rates from models A, B and C at a temperature of 2000 K. It can be seen that the traditional approach, model A, cannot explain the observation of any emission from states with $j \geq 3$. Models B and C do predict some emission, but with fluxes significantly less than those observed. The model results do not compare well with the observations, predicted emission for states with $j > 2$ being, at best, a factor of ≈4 below those observed.

The inferred physical conditions in NGC 7027 quoted above result in a low electron density of $n_e \approx 30\,cm^{-3}$. It is, however, possible that regions of higher electron density may exist due to shocks or photodissociation regions (PDRs), and that some or all of the observable emission from CH^+ originates in such regions. In addition, Cernicharo et al. (1997) interpret their observations in terms of LTE and a rather low fixed temperature of 150 K, which does not appear consistent with the critical densities quoted above and may not be appropriate for the conditions in NGC 7027. To explore this possibility, we also investigate the behaviour of models A, B and C with respect to variations in electron density between $30\,cm^{-3}$ and a maximum of $10^5\,cm^{-3}$. This maximum is derived from a value of $n(H_2) = 5 \times 10^7\,cm^{-3}$ (used by Cernicharo et al. 1997 to explain CH^+ rotational line ratios with H_2–CH^+ collisions) and a warm PDR electron fraction of $n_e/n(H) \approx 10^{-3}$. It does seem likely, however, that this density is an overestimate (Liu et al. 1996; Liu 1997).

Model A again produces a very low amount of excitation; however, models B and C enter regimes of high excitation once the electron density approaches values of order $10^4\,cm^{-3}$. Table 4

Table 3. Predicted steady-state emission fluxes at a $T_E = 2000$ K and $n_e = 30\,cm^{-3}$. Units are number rate of emissions relative to the $j = 2$–1 transition. Observations are from Cernicharo et al. (1997).

Transition:	j = 1-0	j = 2-1	j = 3-2	j = 4-3	j = 5-4	j = 6-5	j = 7-6
Model A:	629.4	1.0	0.0001	0.0	0.0	0.0	0.0
Model B:	1.340	1.0	0.408	0.363	0.146	0.139	0.002
Model C:	1.328	1.0	0.412	0.363	0.147	0.139	0.003
obs:	-	1.0	1.35 ± 0.11	1.23 ± 0.13	0.93 ± 0.15	0.75 ± 0.10	-

Table 4. Predicted steady-state emission fluxes for a range of electron densities. Units are number rate of emissions relative to the $j = 2$–1 transition.

n_e cm^{-3}	j = 1-0	j = 2-1	j = 3-2	j = 4-3	j = 5-4	j = 6-5	j = 7-6
Model B, T = 1000 K							
3.0(1)	1.35	1.00	0.33	0.30	0.10	0.09	0.001
1.0(2)	1.35	1.00	0.33	0.30	0.10	0.09	0.001
5.0(2)	1.33	1.00	0.33	0.30	0.10	0.10	0.001
1.0(3)	1.32	1.00	0.33	0.30	0.10	0.10	0.001
5.0(3)	1.20	1.00	0.34	0.31	0.11	0.10	0.001
1.0(4)	1.08	1.00	0.35	0.32	0.11	0.10	0.001
5.0(4)	0.66	1.00	0.40	0.40	0.14	0.13	0.001
1.0(5)	0.50	1.00	0.45	0.48	0.17	0.17	0.002
Model C, T = 1000 K							
3.0(1)	1.34	1.00	0.34	0.30	0.10	0.09	0.001
1.0(2)	1.30	1.00	0.35	0.30	0.11	0.09	0.002
5.0(2)	1.15	1.00	0.40	0.30	0.12	0.09	0.008
1.0(3)	1.10	1.00	0.46	0.31	0.14	0.09	0.01
5.0(3)	0.50	1.00	0.69	0.36	0.20	0.09	0.03
1.0(4)	0.31	1.00	0.85	0.45	0.26	0.11	0.04
5.0(4)	0.10	1.00	1.69	1.34	0.74	0.34	0.12
1.0(5)	0.07	1.00	2.48	2.60	1.63	0.82	0.28
Model C, T = 2000 K							
3.0(1)	1.33	1.00	0.41	0.36	0.15	0.13	0.002
1.0(2)	1.30	1.00	0.42	0.36	0.15	0.13	0.004
5.0(2)	1.15	1.00	0.47	0.36	0.17	0.13	0.01
1.0(3)	1.00	1.00	0.51	0.37	0.18	0.13	0.02
5.0(3)	0.51	1.00	0.72	0.42	0.26	0.14	0.05
1.0(4)	0.32	1.00	0.87	0.51	0.32	0.15	0.06
5.0(4)	0.10	1.00	1.68	1.41	0.86	0.44	0.17
7.5(4)	0.08	1.00	2.09	2.04	1.31	0.70	0.26
1.0(5)	0.07	1.00	2.46	2.70	1.84	1.01	0.37
obs:	-	1.00	1.35 ± 0.11	1.23 ± 0.13	0.93 ± 0.15	0.75 ± 0.10	-

gives results for a number of such runs. For an electron temperature of 1000 K, it can be seen that transitions other than just those from the $j = 0$ level are of much greater importance than in the low-electron-density models. This is to be expected, since the ground rotational state no longer contains the overwhelming majority of the CH^+ population. For example, an electron density of 75 000 cm^{-3} and temperature of 2000 K in model C produces fractional populations of 0.067, 0.26, 0.35, 0.20, 0.08, 0.03, 0.0079 and 0.0018 for the $j = 0$–7 levels respectively.

For an electron density of order 10^5 cm^{-3}, which roughly corresponds to total carbon ionization, the $j = 6 - 5$ emission rate from model C exceeds that inferred from the observations. However, the emission rates from the lower transitions are too high by factors close to 2. Results from model C for a temperature of 2000 K are shown in Table 4. We find that it is possible to approach the observed rotational line ratios using a model which consists solely of inelastic electron collisions; however, electron densities of the order of 5×10^4 cm^{-3} are required.

Other processes exist which may augment the level populations of CH^+. Cernicharo et al. (1997) suggest molecular hydrogen as an inelastic collision partner for CH^+. However, although detailed rotational excitation rates for H_2–CH^+ collisions are not accurately known, these are undoubtedly orders of magnitude below those for electrons, and it is unlikely that CH^+ can be maintained in LTE in this fashion. Very recently, Black (1998) has proposed a model based on the absorption of locally produced far-infrared radiation. This model gives reasonable agreement with the observed emissions. Our models, however, do demonstrate that the higher rotational states of CH^+ can be significantly populated by electron-impact excitation alone. It is therefore probable that at least some of the observed infrared emission from NGC 7027 results from this process. What our models show is that for the high H density assumed by Cernicharo et al. (1997), electron collisions, ignored by these workers, will significantly affect the CH^+ rotational population.

Finally, it is interesting to note that for $n_e > 10^2$ cm^{-3} our predicted ratio of emission fluxes for $j = 1 - 0$ at 359 μm (Carrington & Ramsay 1982) to $j = 2 - 1$ at 179.61 μm is much more sensitive to electron density than the ratio of higher transitions to $j = 2 - 1$. This suggests that observation of this ratio could yield important information on electron densities in a region where electron collisions control the population of CH^+ rotational levels.

5 CONCLUSIONS

We have computed electron impact rotational excitation cross-sections and rates for CH^+. The calculations use a more rigorous procedure than previous studies, and find important contributions

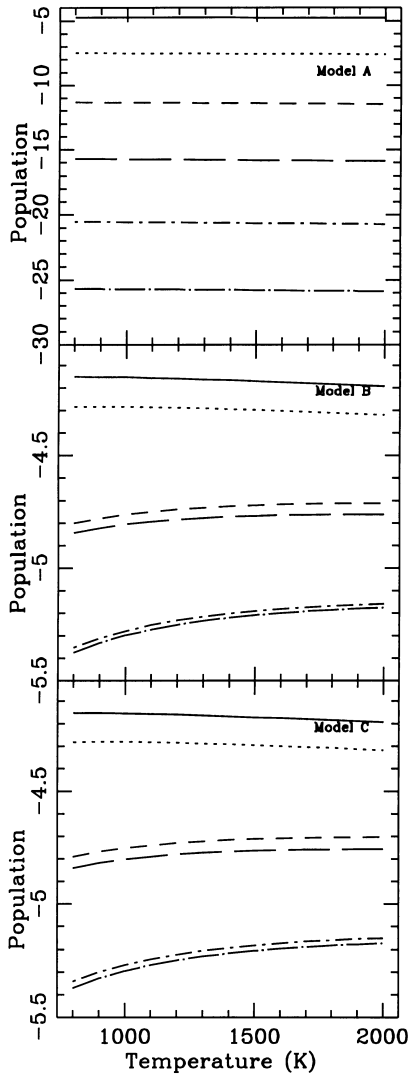

Figure 3. Level populations from models A, B and C for an electron density of $n_e = 30\,\mathrm{cm}^{-3}$ and temperatures between 800 and 2000 K. In top-to-bottom order, the lines represent the populations of levels $j = 1$ (solid line), $j = 2$ (dotted), $j = 3$ (medium-dashed), $j = 4$ (long-dashed), $j = 5$ (dot-dashed) and $j = 6$ (dot/long-dashed).

from transitions with $j > 2$, which have been uniformly neglected in all previous work. In particular, we find that the $\Delta j = 2$ excitation rates actually exceed those for $\Delta j = 1$, the only ones that have previously been considered.

Use of our electron-impact excitation rates in a simple electron collision model of CH^+ rotational populations in NGC 7027 suggest that electron collisions can lead to significant populations of rotational states with $j > 1$, particularly for electron densities of 10^3 or higher.

If electron densities above $10^4\,\mathrm{cm}^{-3}$ can be justified for this nebula, our model suggests that electron collisions alone can explain the high level of CH^+ rotational excitation inferred from the line ratios recently obtained by Cernicharo et al. (1997). Indeed, if we adopt the density values used in the cited paper to explain the observed emission with heavy particle collisions, then we obtain line ratios (relative to the $j = 2$–1 transition) that exceed those observed.

ACKNOWLEDGMENTS

We thank Xiaowei Liu for helpful discussions. This work was supported by the UK Particle Physics and Astronomy Research Council and the Engineering and Physical Sciences Research Council.

REFERENCES

Black J. H., 1998, Faraday Discuss., 109, 257
Boĭkova R. F., Ob"edkov V D., 1968, Sov. Phys. JETP, 27, 772
Cade P. E., Huo W., 1973, At. Nucl. Data Tables, 12, 429
Carrington A., Ramsay D. A., 1982, Physica Scripta, 25, 272
Cernicharo J., Liu X. W., Gonzalez-Alfonso E., Cox P., Barlow M. J., Lim T., Swinyard B. M., 1997, ApJ, 483, L65
Chandra N., Temkin, A., 1976, Phys. Rev. A, 13, 188
Chieze J. P., Pineaux des Forêts G., Flower D. R., 1998, MNRAS, 295, 672
Chu S.-I., Dalgarno, A., 1974, Phys. Rev. A, 10, 788
Dickinson A. S, Flower D. R., 1981, MNRAS, 196, 297
Dickinson A. S, Muñoz J. M., 1977, J. Phys. B: At. Mol. Phys., 10, 3151
Federman S. R., Rawlings J. M. C., Taylor S. D., Williams D. A., 1996, MNRAS, 279, L41
Flower D. R., 1979, A&A, 73, 237
Gillan C. J., Tennyson J., Burke P. G., 1995, in Huo W. M., Gianturco F. A., eds, Computational Methods for Electron–Molecule Collisions. Plenum Press, New York, p. 239
Liu X.-W., 1997, Proc. First ISO Workshop on Analytical Spectroscopy, ESA SP-419, p. 87
Liu X.-W. et al., 1996, A&A, 315, L257
Morgan L. A., Tennyson J., Gillan C. J., 1998, Computer Phys. Commun., 114, 120
Neufeld D. A., Dalgarno A., 1989, Phys. Rev. A, 40, 633
Ornellas F. R., Machado F. B. C., 1986, J. Chem. Phys., 84, 1296
Rabadán I., Tennyson J., 1998, Computer Phys. Commun., 114, 129
Rabadán I., Sarpal B. K., Tennyson J., 1998a, J. Phys. B: At. Mol. Opt. Phys., 31, 2077
Rabadán I., Sarpal B. K., Tennyson J., 1998b, MNRAS, 299, 171
Sarpal B. K., Tennyson J., 1993, MNRAS, 263, 909
Tennyson J., 1988, J. Phys. B: At. Mol. Opt. Phys., 21, 805
Tennyson J., 1996, J. Phys. B: At. Mol. Opt. Phys., 29, 6185
Tennyson J., Burke, P. G., Berrington, K. A, 1987, Computer Phys. Commun., 47, 207

This paper has been typeset from a TEX/LATEX file prepared by the author.